NEOPLASIA
www.neoplasia.com

Volume 18 Number 1 January 2016 pp. 60–70 60

A Novel Mouse Model of Diffuse Intrinsic Pontine Glioma Initiated in Pax3-Expressing Cells[1,2]

Katherine L. Misuraca[*], Guo Hu[*,†], Kelly L. Barton[*,†], Alexander Chung[*,†] and Oren J. Becher[*,†,‡]

*Division of Pediatric Hematology-Oncology, Duke University Medical Center, Durham, NC; †Preston Robert Tisch Brain Tumor Center, Duke University Medical Center, Durham, NC; ‡Department of Pathology, Duke University Medical Center, Durham, NC

Abstract

Diffuse intrinsic pontine glioma (DIPG) is a rare and incurable brain tumor that arises predominately in children and involves the pons, a structure that along with the midbrain and medulla makes up the brainstem. We have previously developed genetically engineered mouse models of brainstem glioma using the RCAS/Tv-a system by targeting PDGF-B overexpression, p53 loss, and H3.3K27M mutation to Nestin-expressing brainstem progenitor cells of the neonatal mouse. Here we describe a novel mouse model targeting these same genetic alterations to Pax3-expressing cells, which in the neonatal mouse pons consist of a Pax3 +/Nestin +/Sox2 + population lining the fourth ventricle and a Pax3 +/NeuN + parenchymal population. Injection of RCAS-PDGF-B into the brainstem of Pax3-Tv-a mice at postnatal day 3 results in 40% of mice developing asymptomatic low-grade glioma. A mixture of low- and high-grade glioma results from injection of Pax3-Tv-a;p53$^{fl/fl}$ mice with RCAS-PDGF-B and RCAS-Cre, with or without RCAS-H3.3K27M. These tumors are Ki67 +, Nestin +, Olig2 +, and largely GFAP − and can arise anywhere within the brainstem, including the classic DIPG location of the ventral pons. Expression of the H3.3K27M mutation reduces overall H3K27me3 as compared with tumors without the mutation, similar to what has been previously shown in human and mouse tumors. Thus, we have generated a novel genetically engineered mouse model of DIPG, which faithfully recapitulates the human disease and represents a novel platform with which to study the biology and treatment of this deadly disease.

Neoplasia (2016) 18, 60–70

Introduction

Brainstem glioma (BSG) is a rare type of brain tumor that arises in the brainstem of predominately children. The brainstem consists of the midbrain, the pons, and the medulla, and whereas low-grade BSG can occur anywhere in the brainstem, high-grade BSG, also known as diffuse intrinsic pontine glioma (DIPG), accounting for 85% of all BSGs, occurs primarily in the pons [1,2]. These tumors are incredibly aggressive, are not amenable to surgery, and have an overall median survival of less than 1 year, with less than 20% of patients alive 2 years after diagnosis [1,2]. The standard treatment regimen of radiation therapy provides only temporary relief from symptoms, and no chemotherapy has shown efficacy over radiation alone for these children [1,2].

Based on large-scale analyses of patient samples in recent years, the genetic alterations characterizing DIPG are being elucidated. These alterations include most notably a K27M mutation in the majority of patients occurring in the gene encoding either histone H3.1 or H3.3, with the latter being more common and associating with a worse prognosis [3–7]. In addition, alterations have been documented in the *PDGFRA* gene (36%), other genes involved in the receptor tyrosine

Address all correspondence to: Oren J. Becher, MD, Assistant Professor, Department of Pediatrics, Duke University Medical Center, 308 Research Dr, LSRC B362, Durham, NC 27710.
E-mail: misuracak@gmail.com

[1] O. J. B. is supported by the Damon Runyon Cancer Research Foundation, U.S. Department of Defense, Rory David Deutsch Foundation, and Pediatric Brain Tumor Foundation. Research reported in this publication was supported by the National Institute of Neurological Disorders and Stroke of the National Institutes of Health under award number K02NS086917.
[2] Conflict of interest: The authors declare that they have no conflict of interest.
Received 20 July 2015; Revised 3 December 2015; Accepted 11 December 2015

1476-5586
http://dx.doi.org/10.1016/j.neo.2015.12.002

kinase PI3K pathway (including *MET* and *PIK3CA*), and genes that regulate RB phosphorylation and the cell cycle [8–13]. Mutations have been discovered in *ACVR1* in roughly 20% of patients [14–17], as well as in *ATRX*, *PPMID*, and *TP53*, the last of which occurs in upwards of 77% of patients [3,17].

Although much work has been accomplished characterizing the genetic basis of DIPG, less research has focused on determining the cell of origin for this disease. Monje et al. [18] has suggested a Nestin+/Vimentin+/Olig2+ cell in the ventral pons during early childhood as a candidate cell of origin based on its peak incidence coinciding with that of DIPG in patients, which would be consistent with the predominantly ventral pontine location of human DIPG [19]. In addition, a recent analysis of the postnatal human pons observed two distinct Nestin+/Vimentin+ populations, one in the dorsal ventricular surface, which persists throughout childhood, and one in the brainstem parenchyma, which disappears by 7 months of age [20]. This same study revealed that a large percentage of the proliferating cells during early childhood in the pons are Olig2+, which could suggest an oligodendroglial origin for DIPG [20], although the possibility remains that DIPG could originate from a nonproliferative cell or a cell during fetal development.

Transgenic mouse modeling using the RCAS/Tv-a system has shown that Nestin-expressing progenitor cells in the P3-P5 mouse brainstem are capable of serving as a cell of origin for BSG when exposed to ectopic PDGF-B ligand and p53-deficiency [21,22] as well as overexpression of H3.3K27M [23]. This model most likely targets Nestin-expressing cells located on the floor of the fourth ventricle [22], although Nestin cells exist throughout the brainstem parenchyma in the P3 mouse brainstem as well [24]. It remains to be seen whether other types of progenitor cells in the neonatal mouse brainstem can support the growth of glioma in mouse models. We have recently identified several regions of Pax3 expression, marking novel populations of cells [24]. We find here that there are at least two distinct types of Pax3 cells in the neonatal mouse brainstem, including an immature Pax3+/Nestin+/Sox2+ progenitor and a more differentiated Pax3+/NeuN+ neuron. To investigate the potential for these cells to be transformed into glioma, we used the Pax3-Tv-a transgenic mouse line [25] to target PDGF-B, H3.3K27M, and p53 loss to Pax3-expressing cells. This combination of genetic alterations leads to BSG of variable grades and latencies, arising anywhere within the brainstem, including the classic DIPG location of the ventral pons. This work describes a novel model of DIPG, which phenotypically resembles the human disease and can be used to further investigate the biological basis of brainstem gliomagenesis and as a preclinical tool to evaluate potential therapeutics.

Materials and Methods

Mice

Nestin-Tv-a mice have been previously described [26]. Pax3-Tv-a mice and their genotyping have been described [25]. Pax3-Tv-a (Ptv-a) mice were bred with $p53^{fl/fl}$ mice (Jackson Labs) to generate Ptv-a;$p53^{fl/fl}$ mice. Nestin-CFPnuc mice have been previously described and express the cyan fluorescent protein (CFP) fused to a nuclear localization signal under the control of the regulatory elements of the Nestin gene [27]. All work with mice was done in accordance with the Duke University Animal Care and Use Committee and the Guide for the Care and Use of Laboratory Animals.

RCAS/Tv-a Glioma Mouse Modeling

The generation of glioma using the RCAS/Tv-a system has been previously described [24]. Pax3-Tv-a mice were injected with DF1 cells producing RCAS viruses at postnatal days 3 and 4 (P3-4) as described, and injected mice were monitored daily and euthanized with CO_2 upon the appearance of signs of brain tumors (enlarged head, ataxia, weight loss up to 25%) or at 12 weeks postinjection in the absence of symptoms. Brains of sacrificed mice were fixed in 10% formalin for at least 24 hours and embedded in paraffin for histological analysis.

Immunofluorescence

Wildtype Nestin-Tv-a or Nestin-CFPnuc mice were sacrificed at P3, and their whole brains were fixed in 4% paraformaldehyde (PFA) in phosphate-buffered saline (PBS) for 24 hours, cryopreserved in 30% sucrose in PBS for 24 to 48 hours, and embedded in ornithine carbamoyltransferase on dry ice/ethanol. Blocks were sectioned using either a Shandon or Leica Cryostat into 12-μm–thick sections in a sagittal orientation. Sections were rehydrated in PBS-T (0.1% Triton-X100) and blocked in PBS-T with 10% normal goat serum. Primary antibodies were diluted in PBS-T with 1% BSA and incubated overnight at 4°C, and secondary antibodies were diluted in PBS-T and incubated for 1 hour at room temperature. Antibodies used were anti-PAX3 (DSHB, mouse IgG2a, concentrated form, 1:200), anti-Ki67 (BD Pharmingen, mouse IgG1, #556003, 1:100), anti-Olig2 (Millipore, anti-rabbit IgG, #AB9610, 1:500), anti-NeuN (Millipore, mouse IgG1, #MAB377, 1:100), anti-Sox2 (Millipore, rabbit, #AB5603, 1:100), anti-Nkx2.2 (DSHB, mouse IgG2b, #74.5A5, concentrated form, 5 μg/ml), and anti-GFP (Invitrogen, 1:200). AlexaFluor goat anti-mouse IgG2a-594, goat anti-mouse IgG1-488, goat anti-mouse IgG2b-488, and goat anti-rabbit-488 secondary antibodies (Invitrogen) were used at 1:500. Slides were mounted with Vectashield with 4',6-diamidino-2-phenylindole (DAPI) (Vector Laboratories) and imaged using a Zeiss Axio Imager. Quantification of the percentage of Pax3+ cells that are Nestin+ was done as previously described using Nestin-CFPnuc mice [24].

Tumor Grading and Immunohistochemistry

Tumor samples fixed in 10% formalin were embedded in paraffin by the Duke Pathology Core and cut into 5-μm–thick sections using a Leica RM2235 microtome. Hematoxylin and eosin (H&E) staining was performed using standard protocols. Tumor grading was done using the following criteria: low-grade glioma (grade II) was indicated by an increased cellular density and the presence of Ki67+ cells; high-grade glioma (grades III and IV) was indicated by the presence of microvascular proliferation and/or the presence of pseudopalisading necrosis. Immunohistochemistry (IHC) was performed using an automated processor (Discovery XT, Ventana Medical Systems, Inc.). Antibodies used were anti-Olig2 (Millipore, #AB9610, 1:500), anti-GFAP (Dako, #Z0334, 1:2,000), anti-Nestin (BD Pharmingen, #556309, 1:200), anti-Ki67 (Abcam #ab16667, 1:200), anti-HA (Santa Cruz Biotechnology, #SC-805, 1:250), and anti–Tri-Methyl-Histone H3 Lys27 (Cell Signaling, #C36B11, 1:200). For rabbit antibodies, 10% normal goat serum in 2% BSA was used for the option/blocking step, and biotinylated goat anti-rabbit IgG (Vector Laboratories, #BA-1000, 1:300) was used for detection. For mouse antibodies, the Mouse on Mouse Basic Kit (Mouse on Mouse, Vector Laboratories, #BMK-2202) was used as directed for the option/blocking and detection steps.

Quantification of H3K27me3 Levels

For each tumor sample analyzed, staining for H3K27me3 was performed on the Discovery (Ventana Medical Systems, Inc.) in the same run. At least 10 40 × pictures were taken of random fields within each tumor. The H3K27me3-positive nuclear area (homogenously staining brown) and total nuclear area per field were quantified using MetaMorph Premier software. A threshold was established to include the H3K27me3-positive nuclei, and then Integrated Morphometry Analysis (with a minimum size of 1000) was used to quantify the positive nuclear area. A threshold was then established for total nuclear area, and then Region Statistics was used to quantify the thresholded area. H3K27me3-positive nuclear area was normalized to total nuclear area for each field, and the mean for each tumor was calculated. The comparison between PDGF-B + Cre and PDGF-B + H3.3K27M + Cre groups was conducted using GraphPad Prism software and the unpaired *t* test.

Results

Characterization of Pax3-Expressing Cells in the Neonatal Mouse Brainstem

We have previously reported the existence of Pax3-expressing cells in the neonatal mouse brainstem, with populations located in the ventral, mid, and dorsal pons, as well as the midbrain and floor of the fourth ventricle [24]. In addition, Pax3-expressing cells are found in the dorsal-most region of the murine thalamus and the internal granule layer of the cerebellum (Figures S1 and S2). Whereas all of the Pax3-expressing cells in the fourth ventricle lining coexpress the neural stem and progenitor cell marker Nestin [24], the majority of Pax3 cells in the midbrain, pons, and thalamus are Nestin negative (Figures 1*A* and S1), suggesting the existence of at least two distinct types of Pax3 cells (Nestin+ and Nestin−). We find here that, in addition to Nestin, the Pax3+ cells lining the fourth ventricle also express Sox2, another early neural stem/progenitor cell marker, and are occasionally found proliferating based on Ki67 staining (Figure 1, *B–E*). This is similar to the Pax3+ cells found in the internal granule layer of the cerebellum, a subset of which also coexpresses Nestin, Sox2, or Ki67 (Figure S2).

In contrast to the immature Pax3 progenitor cells found lining the fourth ventricle, those in the pons parenchyma are largely Nestin negative, with the exception of less than 5% of Pax3 cells in the dorsal pons (Figure 1*A*); Sox2 negative (Figure 2, *A* and *E*); and Ki67 negative (Figure 2, *B* and *F*). Pax3-expressing cells in the pons are not of the oligodendrocyte lineage based on Olig2 and Nkx2.2 staining (Figure 2, *C–D* and *G–H*; positive Nkx2.2 staining in the midbrain is shown in Figure S3*A*). We do, however, find that a subset of the Pax3-expressing cells in the pons expresses the neuronal lineage-specific marker NeuN (Figure 3). Those residing in the ventral pons express relatively high levels of NeuN (Figure 3, *A–F*), whereas those in the

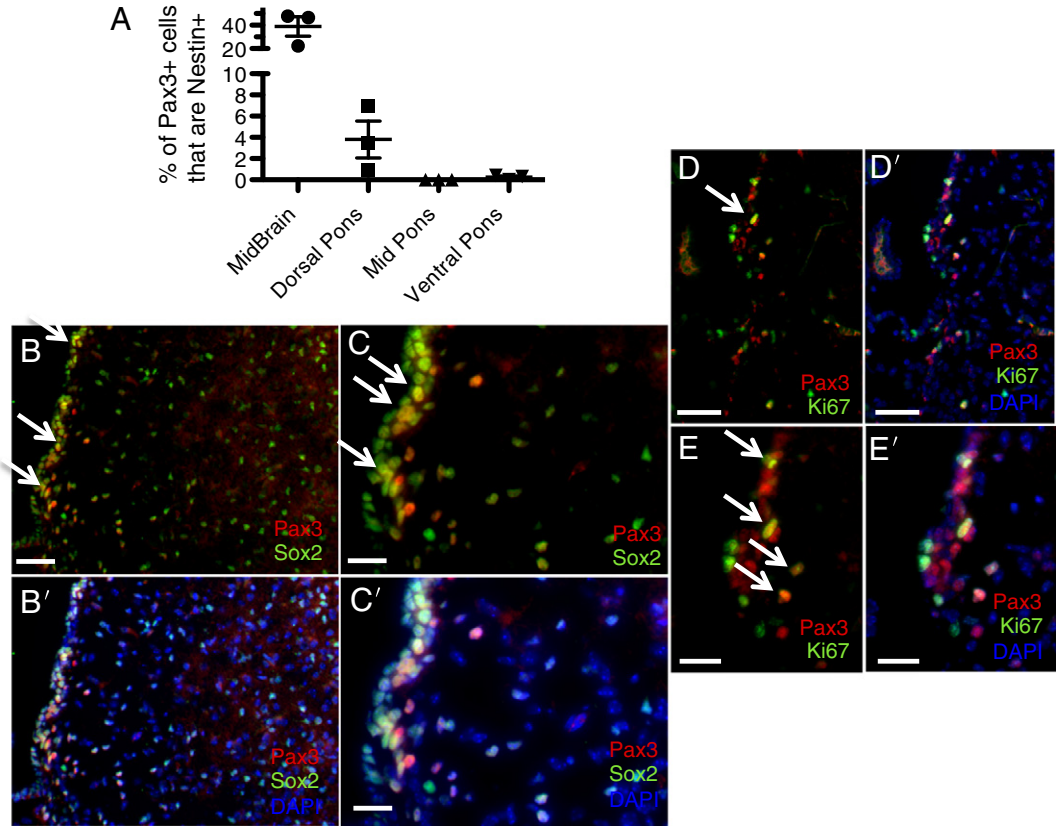

Figure 1. Pax3-expressing progenitor cells in the neonatal mouse brainstem. (A) Coimmunofluorescence for Pax3 and Nestin-CFP (using a GFP antibody) was conducted in P3 sections of Nestin-CFPnuc brainstem, and the percentage of Pax3+ cells in each of the indicated brainstem regions that were also Nestin+ was calculated as described in the Materials and Methods and in [24]. (B–D) Coimmunofluorescence of wild-type P3 mouse brainstem for Pax3 and Sox2 (B and C) or Ki67 (D and E). DAPI counterstain is shown in (B′–E′) to indicate total nuclei. 20× magnification (B and D), scale bar is 50 μm; 40× magnification (C and E), scale bar is 25 μm. White arrows point to examples of double-positive cells.

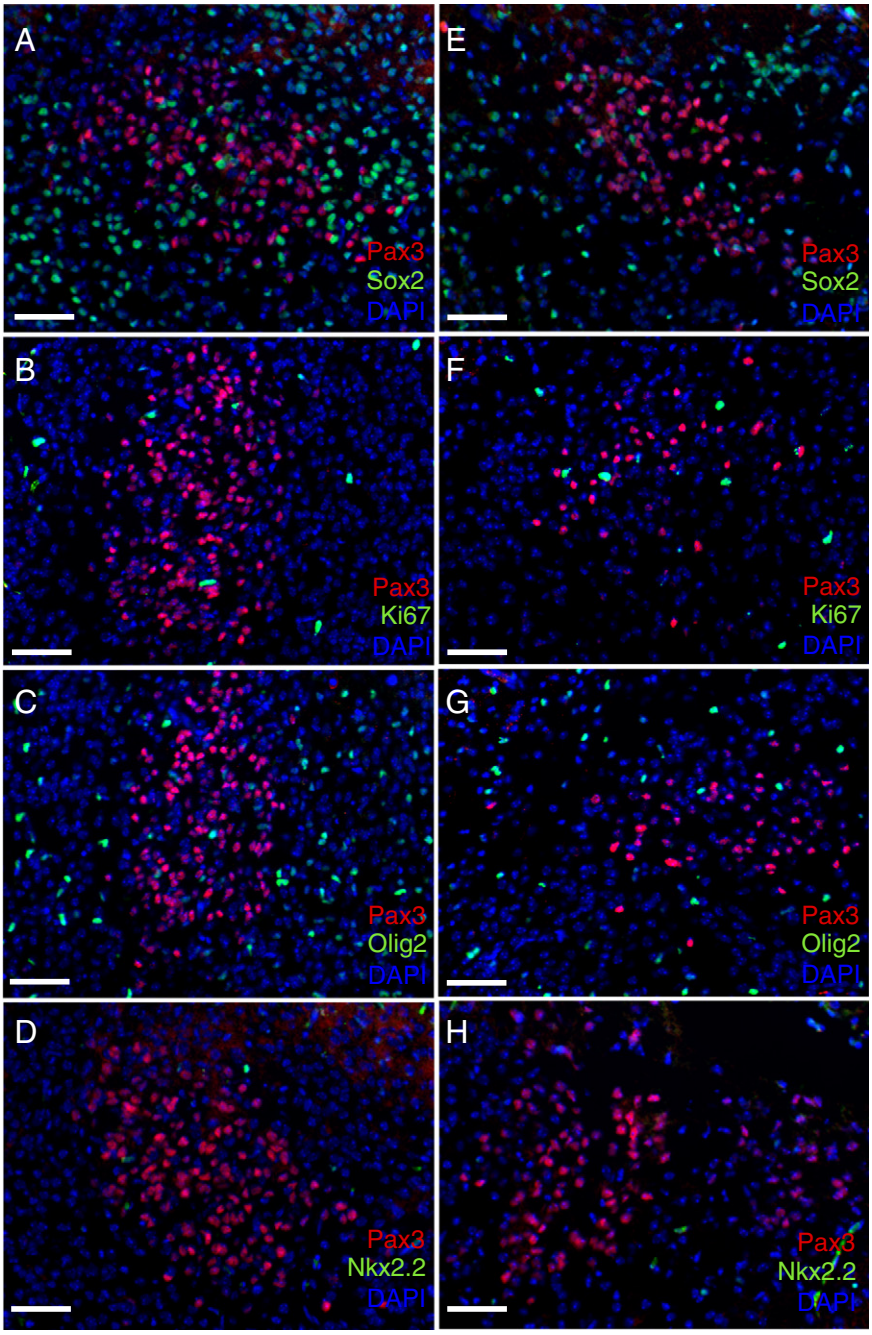

Figure 2. Pax3-expressing cells in the neonatal mouse pons. Coimmunofluorescence of wild-type P3 mouse dorsal pons (A–D) and ventral pons (E–H) for Pax3 and Sox2 (A and E), Ki67 (B and F), Olig2 (C and G), and Nkx2.2 (D and H). DAPI counterstain is shown to indicate total nuclei. 20× magnification, scale bar is 50 μm.

dorsal pons express lower levels of NeuN (Figure 3, *G–L*), suggesting that these cells belong to the neuronal linage. This is similar to the Pax3 cells in the dorsal thalamus, a subset of which expresses NeuN (Figure S1), but is in contrast to the Pax3 cells in the cerebellum, which do not express NeuN (Figure S3*B*).

PDGF-Driven Brainstem Glioma Initiated in Pax3-Expressing Cells

We have previously shown that targeting Nestin progenitor cells in the neonatal mouse brainstem with PDGF-B overexpression induces high-grade glioma formation in conjunction with Ink4aARF-loss or p53-loss and H3.3K27M overexpression [21–24]. Although a small percentage of the Nestin progenitors in the neonatal brainstem also express Pax3 and we may be infecting some of these double-positive cells in the Nestin-derived mouse model [24], we were interested in determining whether Pax3-expresing cells could serve as a cell of origin for BSG regardless of their Nestin expression.

To test this, we used a Pax3-Tv-a (Ptv-a) transgenic mouse, which expresses the Tv-a receptor under the control of the Pax3 promoter [25]. Ptv-a mice were injected with RCAS-PDGF-B–producing cells at P3-4 and were monitored for signs and symptoms of brain tumors. These mice did not develop any symptoms of brain tumors and were

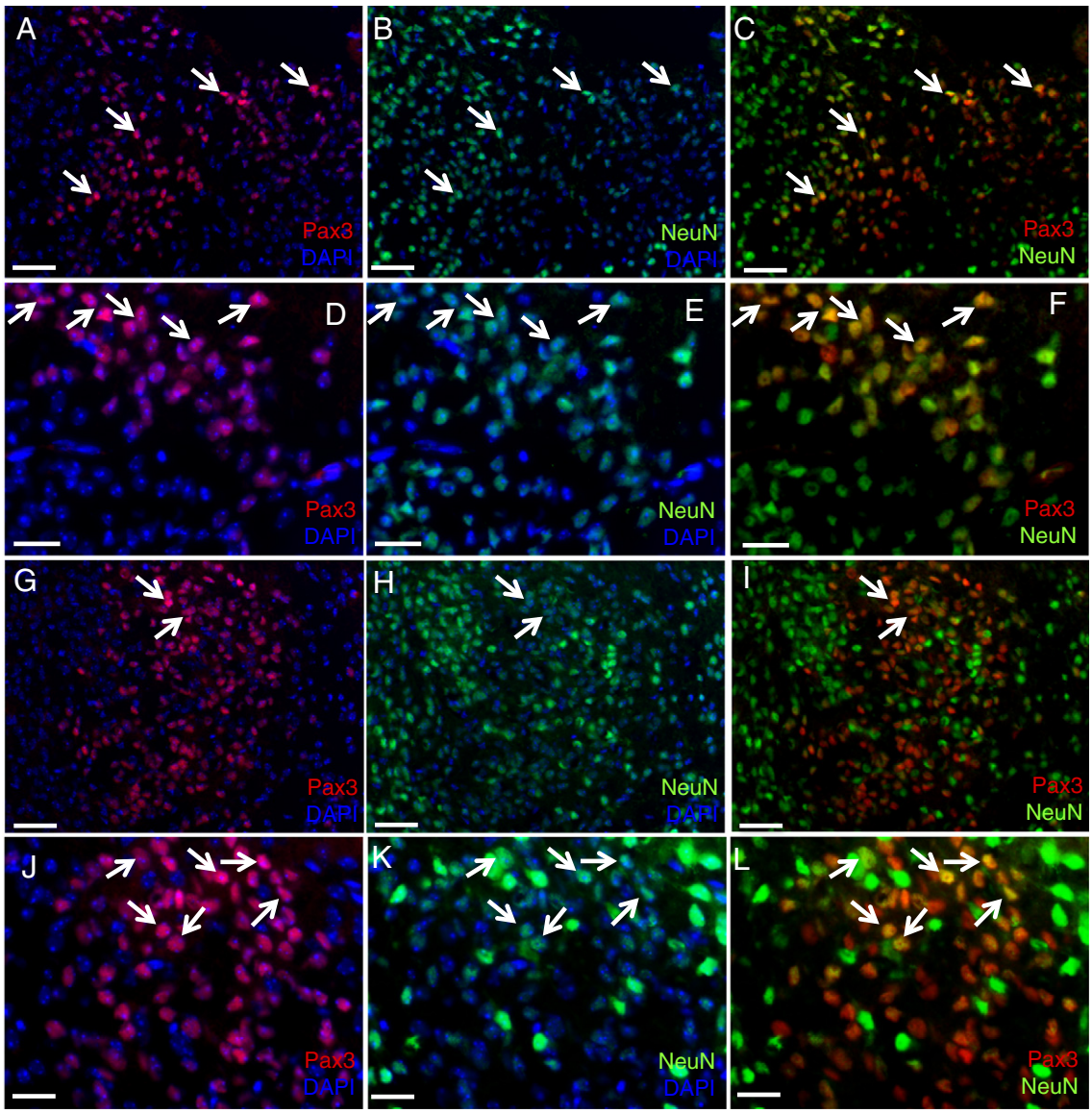

Figure 3. Pax3-expressing progenitors in the neonatal mouse pons express NeuN. Coimmunofluorescence of wild-type P3 mouse ventral pons (A–F) and dorsal pons (G–L) for Pax3 (red) and NeuN (green). DAPI counterstain (blue) is shown in some panels to indicate total nuclei. 20× magnification (A–C and G–I), scale bar is 50 μm. 40× magnification (D–F and J–L), scale bar is 25 μm. (J–L) The NeuN signal (green) is enhanced relative to other panels to highlight the double-positive cells. White arrows point to double-positive cells.

sacrificed at 12 weeks postinjection to investigate the occurrence of low-grade gliomas (Figure 4*A*). Four out of seven mice (42.9%) showed evidence of low-grade lesions in the brainstem based on the presence of small clusters of proliferating Ki67 + cells (Figure 4, *B* and *C*).

We next crossed the Ptv-a mice with p53-floxed mice and injected the resulting Ptv-a;p53$^{fl/fl}$ mice with either RCAS-PDGF-B + RCAS-Cre or RCAS-PDGF-B + RCAS-Cre + RCAS-H3.3K27M at P3-4. Roughly 50% of the injected mice developed symptoms of brain tumor formation between 34 and 83 days postinjection (Figure 4*A*), with the remaining mice sacrificed at 12 weeks. All mice were processed for immunohistochemical analysis. Based on H&E and Ki67 staining, 10 of 12 mice (83.3%) injected with PDGF-B and Cre developed BSG of variable grades (25% low grade and 58.3% high grade; Figures 4, *B* and *D*, and 5*A*), whereas 11 out of 15 mice (73.3%) injected with PDGF-B, Cre, and H3.3K27M developed glioma (20% low grade and 53.3% high grade; Figures 4, *B* and *E*, and 5, *B* and *C*). Staining for HA (a tag that marks both the RCAS-PDGF-B and RCAS-H3.3K27M constructs) shows primarily cytoplasmic expression in the PDGF-B; p53-deficient tumors (Figure 4*D*) and predominately nuclear expression in the PDGF-B; H3.3K27M; p53-deficient tumors (Figure 4*E*), indicating successful expression of the H3.3K27M oncoprotein in the latter tumors. The gliomas arose in variable locations throughout the brainstem, including the ventral pons, dorsal pons, midbrain, and lining of the fourth ventricle, and occasionally invaded into the cerebellum (Figure 5). Tumor cells were also sometimes found within the fourth ventricle, spreading to other ventricular spaces throughout the brain and consequently invading into the parenchyma elsewhere in the brain, evidence of leptomeningeal disease (Figure S4).

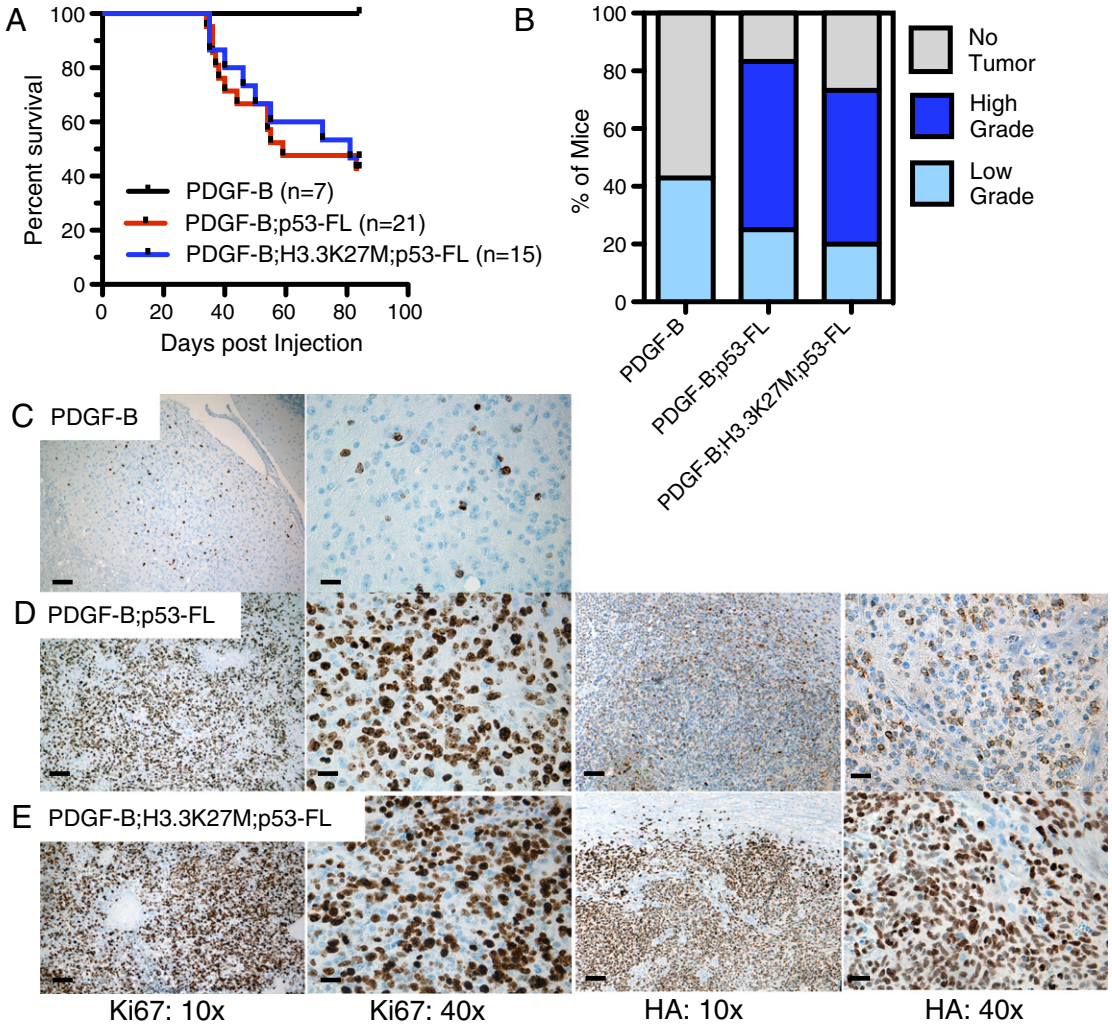

Figure 4. BSG initiated in Pax3-Tv-a mice. (A) Kaplan-Meier survival curve of Pax3-Tv-a (Ptv-a) mice injected with DF1 cells expressing RCAS-PDGF-B, RCAS-PDGF-B+RCAS-Cre, or RCAS-PDGF-B+RCAS-Cre+RCAS-H3.3K27M. (B) Mice from (A) were sacrificed at the onset of tumor symptoms or at 12 weeks in the absence of symptoms. Brains were harvested, fixed in formalin, and analyzed for the presence of tumors using H&E staining, and the tumors were graded as described in the Materials and Methods. Shown is the percentage of mice in each group with no tumor, low-grade glioma (II), and high-grade glioma (III-IV). (C–E) Representative IHC of low-grade BSG driven by PDGF-B (C, Ki67), high-grade BSG driven by PDGF-B and Cre (D, left panels are Ki67 and right panels are HA), and high-grade BSG driven by PDGF-B, Cre, and H3.3K27M (E, left panels are Ki67 and right panels are HA); 10× magnification, scale bar is 100 μm; 40× magnification, scale bar is 25 μm.

The high-grade gliomas induced in this model harbor a high proliferative index (Figure 4, *D* and *E*) and microvascular proliferation and/or pseudopalisading necrosis (Figure 5). These tumors express the glioma markers Nestin and Olig2 in the majority of tumor cells (Figure 6, *A–B* and *D–E*). The glioma marker GFAP is less prominently expressed in these tumors, seemingly characterizing cells in the perivascular niche only and not marking the majority of tumor cells (Figure 6, *C* and *F*).

Leptomeningeal Lesions Induced by Injections into the Cerebral Cortex of Pax3-Tv-a Mice

As a control, Ptv-a;p53$^{fl/fl}$ mice were injected into the cerebral cortex at P3 with RCAS-PDGF-B and RCAS-Cre to ascertain whether this model can be used to study gliomas of the cerebral cortex as well. As there is no Pax3 expression in the parenchyma of the cerebral cortex at this developmental stage [24], we did not expect these mice to develop glioma. Surprisingly, 3 of 9 mice (33%) developed symptoms of brain tumors before the 12-week end point including lethargy, enlarged head, and paralysis in one case, which necessitated sacrificing (Figure S5*A*). The remaining 6 mice were sacrificed at 12 weeks postinjection. All brains were cut in the coronal orientation, fixed in formalin, and embedded in paraffin for histological examination. Based on H&E and Ki67 staining, no brains displayed any evidence of glioma formation within the cerebral cortex parenchyma; however, four of nine brains harbored enlarged ventricles as a consequence of hydrocephalus (Figure S5, *B* and *C*), and three of nine brains harbored small leptomeningeal lesions within the lateral ventricles of the cerebral cortex (Figure S5, *D–I*). These lesions were presumably responsible for the hydrocephalus and symptoms that developed in these mice.

Reduction in Global H3K27me3 Induced by the Ectopic Expression of H3.3K27M in Pax3-Expressing Cells

The ectopic expression of H3.3K27M does not alter the latency or penetrance of tumor formation driven by PDGF-B overexpression

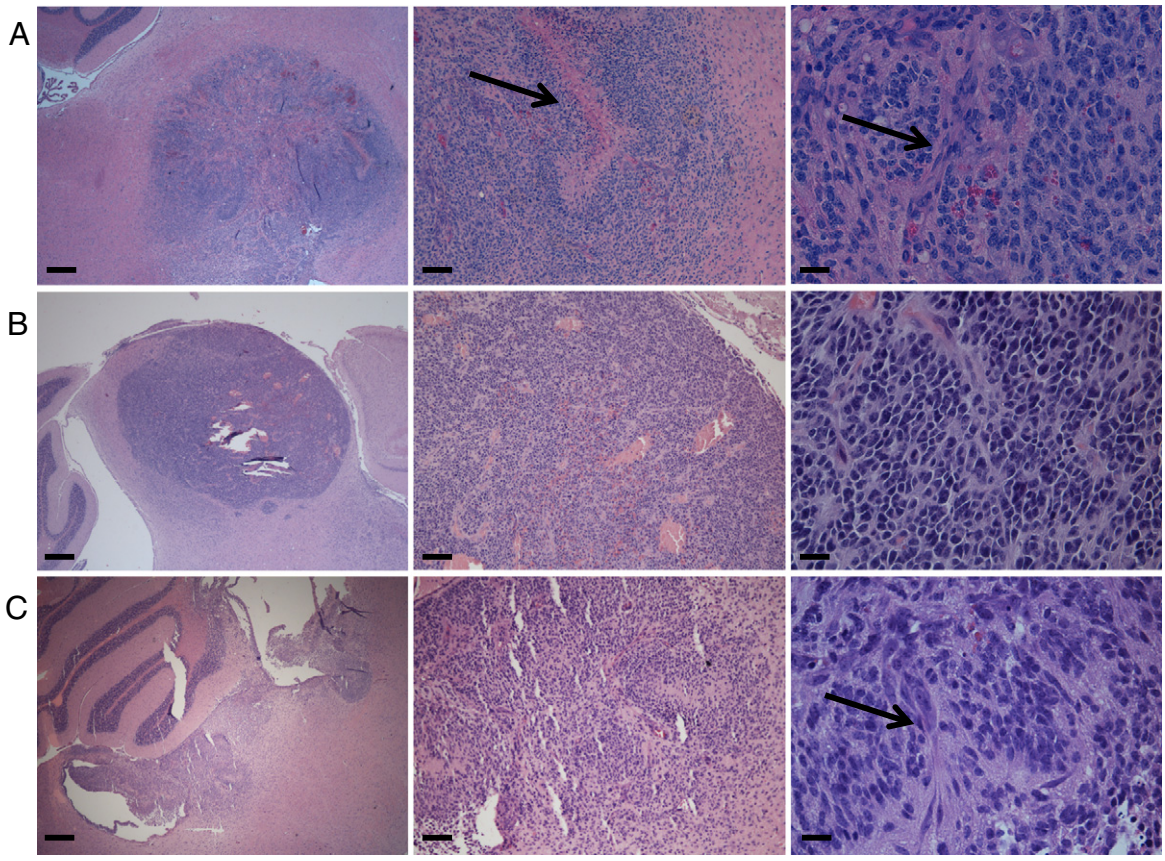

Figure 5. Gliomas initiated in Pax3-Tv-a mice can arise throughout the brainstem. Representative H&E staining of high-grade BSG initiated in Pax3-Tv-a mice by PDGF-B and Cre (A) or by PDGF-B, Cre, and H3.3K27M (B-C), occurring in the ventral pons (A), midbrain (B), and dorsal pons, involving the fourth ventricle and cerebellum (C). Magnification in left panels is 2.5×, scale bar is 400 μm; magnification in middle panels is 10×, scale bar is 100 μm; magnification in right panels is 40×, scale bar is 25 μm. Arrows in (A) indicate pseudopalisading necrosis in the middle panel and microvascular proliferation in the right panel. Arrow in (C) indicates microvascular proliferation in the right panel.

and p53 loss in Pax3-expressing cells (Figure 4, *A* and *B*), nor does it alter the tumors' phenotypic profiles (Figure 6). Immunohistochemical staining for the H3K27me3 mark in PDGF-B + p53-loss tumors showed variable staining within individual tumors, with areas of high levels of H3K27me3 (Figure 7*A*) and areas of low or no H3K27me3 (data not shown). Ectopic expression of H3.3K27M, however, significantly reduced the presence of this trimethyl mark in the tumors (Figure 7*B*). Quantification of the overall levels of H3K27me3 nuclear area relative to total nuclear area per high-powered field in these two groups of tumors showed a significant reduction in H3K27me3-positive nuclear area in H3.3K27M-expressing tumors (PDGF-B+Cre mean = 1.3 ± 0.2% [SE], n = 7; PDGF-B+H3.3K27M+Cre, mean = 0.4 ± 0.15% [SE], n = 7; P = .0056 by unpaired t test; Figure 7*C*).

Discussion

With the increased availability of DIPG biopsy and autopsy material in recent years, our understanding of the biological basis of this rare disease is beginning to catch up to that of other types of glioma. In addition, these human samples are now being used to develop patient-derived orthotopic xenograft models [28] for the study of DIPG (reviewed in [29]), models that accurately represent the human disease and harbor human cells growing in the appropriate location. However, studies of DIPG using patient-derived orthotopic xenograft models must be complemented by studies using genetically engineered mouse models (GEMMs), as GEMMs represent primary tumors growing in their native microenvironment with defined genetic alterations and in the presence of an intact immune system. Despite this, there remains a paucity of GEMMs with which to study the initiation, progression, and treatment of DIPG. Here we describe a novel GEMM of DIPG that is initiated in Pax3-expressing cells. Pax3 is a transcription factor that shows a regional expression pattern throughout central nervous system development, beginning with the embryonic neural tube in which it characterizes the dorsal half of the neural tube and inhibits p53-dependent apoptosis [30–33]. Later in postnatal development, its expression marks dorsal regions of the brain including the brainstem and cerebellum, whereas it is absent from ventral regions such as the cerebral cortex [24,34]. Becasue of this regional expression pattern during development, Pax3 uniquely characterizes gliomas arising in the brainstem of mice and humans, and Pax3 functionally enhances PDGF-B–driven gliomagenesis in mice initiated in Nestin-progenitor cells by inhibiting apoptosis and promoting cell survival and proliferation [24].

Further characterization of Pax3-expressing cells in the developing mouse brainstem shown here revealed that there are at least two distinct populations of Pax3 cells. Dorsal regions of the brainstem, such as the lining of the fourth ventricle, harbor Pax3 expression that

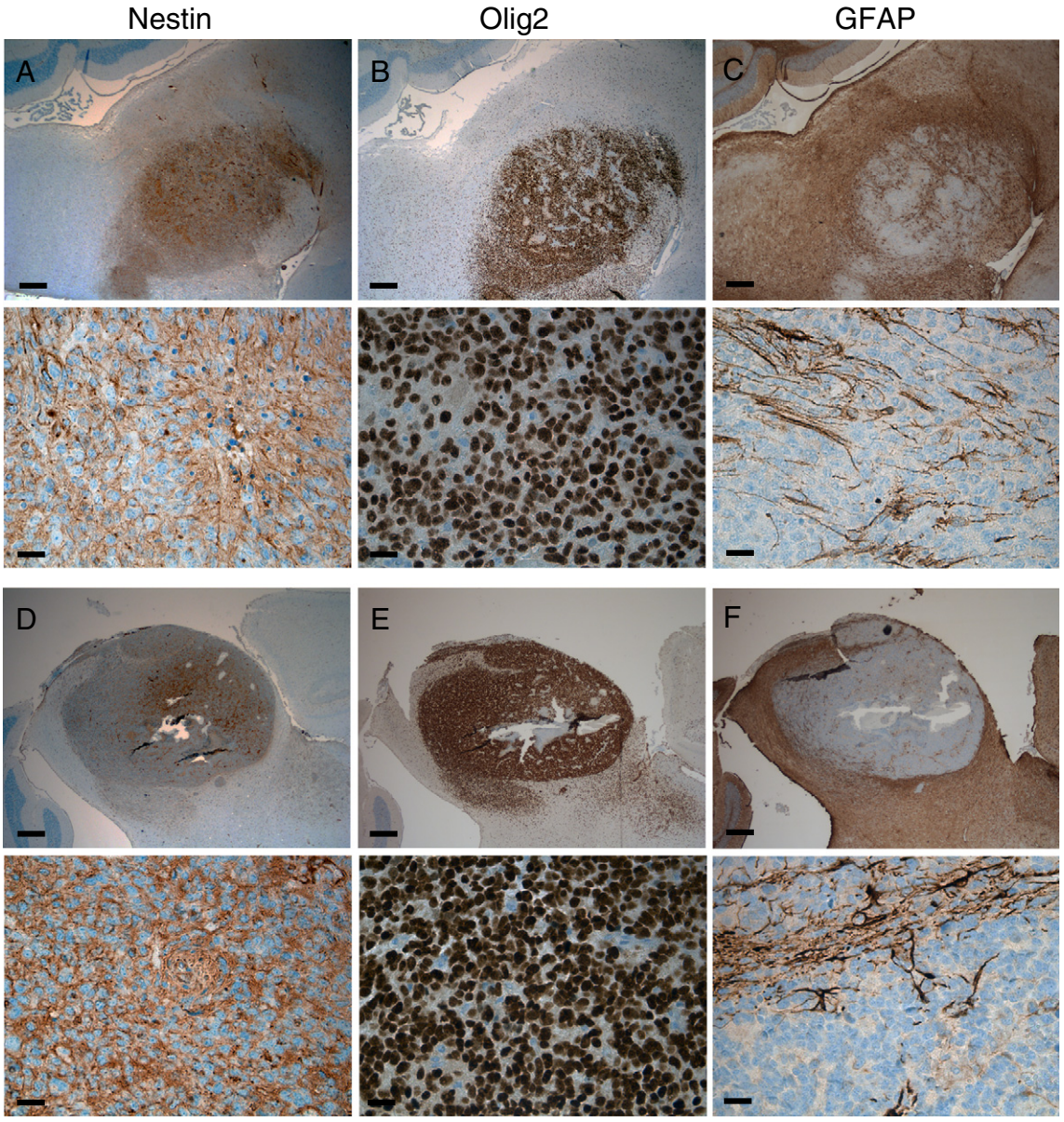

Figure 6. BSGs initiated in Pax3-Tv-a mice. Immunohistochemistry for Nestin (A and D), Olig2 (B and E), and GFAP (C and F) in BSG driven by PDGF-B and Cre (A–C) and PDGF-B, Cre, and H3.3K27M (D–F). Upper panels are 2.5 × magnification, scale bar is 400 μm; lower panels are 40 ×, scale bar is 25 μm.

overlaps partially with Nestin, Sox2, and the proliferation marker Ki67. This suggests that these cells are relatively immature neural progenitor cells. Pax3 cells located in the parenchyma of the pons seem to have a distinct phenotypic profile, being more differentiated in a dorsal to ventral direction. A very small subset of the dorsal pontine Pax3-expressing cells coexpresses Nestin; however, all of these cells lack expression of Sox2 and Ki67, and a subset expresses low levels of the neuronal lineage marker NeuN. These data suggest that a subset of these cells is beginning to differentiate down the neuronal lineage. The ventral pontine Pax3-expressing cells do not express Nestin, Sox2, or Ki67, and a subset expresses higher levels of NeuN. These observations suggest that, in contrast to the relatively immature Pax3 progenitors of the fourth ventricle lining, the Pax3 cells in the pons parenchyma are more differentiated and committed to the neuronal lineage.

When Pax3-expressing cells are targeted for gliomagenesis in Pax3-Tv-a (Ptv-a) mice using PDGF-B and H3.3K27M overexpression along with p53 loss, gliomas arise anywhere in the brainstem, including the ventral and dorsal pons, midbrain, and fourth ventricular space beginning 35 days postinjection. This is an important observation, as the majority of high-grade BSGs, or DIPGs, are located within the ventral pons [19], and so the generation of a model that anatomically resembles DIPG in its location within the brainstem is of extreme value to the field. The varied locations of the tumors in this model are most likely reflective of the variability in injection location inherent in a free-hand injection-based model. Given that there are populations of Pax3-expressing cells lining the fourth ventricle, in the midbrain, and in the pons at P3 and we are able to generate tumors in each of these locations, all of these distinct populations of Pax3 cells may be

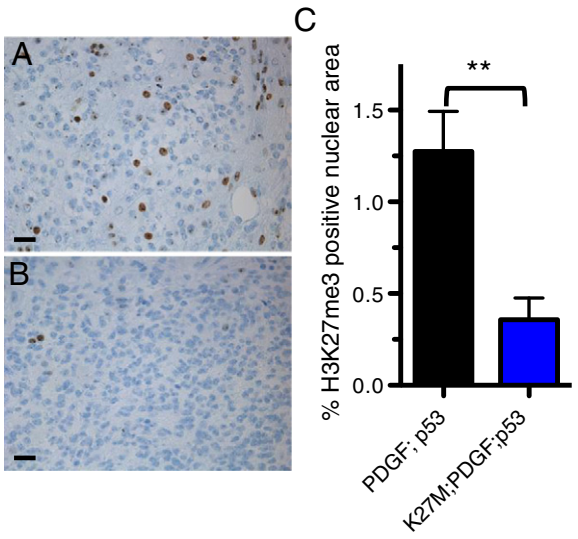

Figure 7. H3.3K27M reduces the prevalence of H3K27me3 in gliomas initiated in Pax3-Tv-a mice. Representative IHC for the H3K27me3 mark in BSG driven by PDGF-B and Cre (A) and by PDGF-B, Cre, and H3.3K27M (B). (C) Quantification of the H3K27m3 mark in BSG driven by PDGF-B and Cre ($n = 7$) and PDGF-B, Cre, and H3.3K27M ($n = 7$); $P = .0056$ by unpaired t test.

capable of serving as a cell of origin for BSG. However, we cannot rule out alternative explanations. For example, the ventral pontine gliomas presumably arise from infection of the ventral pontine Pax3+ neurons; however, it is possible that they arise from infection of fourth ventricular Pax3+ progenitors that migrate into the pons after infection or from Pax3+/NeuN− cells in the pons. We will require additional lineage tracing tools to understand whether there are differences either in the susceptibility to tumorigenesis between these different populations or in the end-stage tumors arising from them.

The tumors in the murine model characterized here are driven by enhanced PDGF signaling and express high levels of Olig2, the latter of which is expressed in more than 90% of DIPGs [35] and both of which characterize the oligodendroglial/PDGFRA and H3-K27M subgroups of human DIPG [5,7,12,36]. Although the H3.3K27M oncoprotein is now considered the hallmark of DIPG, it is interesting to note that, in our PDGF-B:p53-deficient model, its ectopic expression globally reduces the H3K27me3 mark but does not further accelerate the gliomagenesis process. The presence of the H3.3K27M mutation in human patients predicts a significantly poorer outcome [3,7], and *in vitro* and *in vivo* studies have suggested a functional role for the mutation in gliomagenesis [23,37]. In contrast, a recent *in vivo* study showed that the H3.3K27M mutation did not alter tumor volume at the onset of symptoms in the Nestin-Tv-a model [38]. This finding, along with those of the present study, may indicate that the timing of oncogenic events is important (the H3.3K27M mutation may be an early event occurring before alterations in PDGF signaling and p53 mutations in the human disease). Alternatively, it may be the case that the targeted cells in some experiments thus far have been incorrect, and thus Pax3-expressing cells may not be the primary cell of origin for DIPG. K27M-mutant human tumors are also found in the thalamus and spinal cord in addition to the pons [5], and as shown here, we have found Pax3-expressing cells in the murine pons and thalamus (although the spinal cord was not examined), lending credence to the possibility that Pax3-expressing cells are a potential cell of origin for K27M-mutant glioma. Further investigations targeting the H3.3K27M mutation to alternative cells of origin in the murine brainstem may help to clarify this issue.

It will be important in the future to determine whether there are similar populations of Pax3 cells in the developing human brainstem that could represent cells of origin for the human disease. According to the BrainSpan Database (www.brainspan.org), Pax3 does display a regional expression pattern in the human brain throughout all stages of prenatal and postnatal development, similar to what we have found in the mouse, with its expression in the hindbrain region of the cerebellum and absence from the frontal cerebral cortex. Unfortunately, brainstem tissues are currently not included in this database, and it remains to be seen whether Pax3 cells can be identified in the human pons. As the ventral pontine Pax3+ neurons described here are Nestin- and Olig2-negative, if there are Pax3+ cells in the human pons, we presume that they are distinct from the ventral pontine Nestin+ progenitors previously described and speculated to be potential cells of origin for DIPG [18,20]. The Pax3+/Nestin+ progenitors of the fourth ventricle floor described here, though, if found in the human brainstem, may represent an alternative cell of origin either for dorsally located low-grade BSG (as was suggested for the Nestin+ cells of the dorsal pons in [20]) or for high-grade DIPG that may initiate in the dorsal brainstem but upon diagnosis encompasses primarily the ventral pons due to migration of tumor cells. In addition, a focus of future investigations will be to compare genomic, expression, and methylation profiles of the end-stage tumors from this Pax3-Tv-a model with those of other genetically engineered mouse models (Nestin-Tv-a and GFAP-Tv-a), along with human tumors, to determine which model most accurately resembles the human disease.

Despite the occurrence of leptomeningeal lesions in the Pax3-Tv-a model after virus injection into the cerebral cortex, which we speculate is a result of virus-producing cells reaching the lateral ventricles, traveling to the fourth ventricle, and infecting Pax3-expressing cells that line the fourth ventricle, we are unable to generate gliomas in the cerebral cortex parenchyma as is possible with the Nestin-Tv-a model. This phenomenon makes the Pax3-Tv-a model a valuable tool for BSG research, as it is specific to the brainstem. Regional differences in glioma are becoming increasingly apparent [12,39], in particular with respect to differences between DIPG and supratentorial glioma [8,12,13,24], and many have hypothesized and provided preliminary evidence that gliomas in different regions of the brain arise from distinct cells-of-origin characteristic of their particular region [5,24,39]. Therefore, it is interesting to hypothesize that BSG may arise from a distinct type of cell that does not exist in other regions of the brain, such as the Pax3-expressing cells described herein.

This Pax3-Tv-a model of BSG displays a longer latency and lower penetrance as compared with our previously reported Nestin-Tv-a model with PDGF-B and p53 loss [24]. This observation may be due to the infection of different types of cells in the Pax3-Tv-a model that are more differentiated and thus less susceptible to transformation than those targeted in the Nestin-Tv-a model. The differences in differentiation and proliferation status between Nestin+ and Pax3+ cells in the pons may explain the differences noted prospectively between these two models. However, we cannot rule out other factors such as a lower frequency of Pax3-positive cells in the P3 brainstem as compared with Nestin-positive cells, or a background difference between the mouse strains. As with any RCAS-Tv-a model, injection

of the viruses infects multiple cells, and as there are many different types of Pax3 cells present in the P3 brainstem (some of which overlap with Nestin-expressing cells), it is likely that several distinct types of Pax3-expressing cells are infected simultaneously with each injection. An important difference already noted between the models, however, is the fact that cerebral cortex injection into Nestin-Tv-a mice leads to cerebral cortex glioma, whereas similar injection into Pax3-Tv-a mice does not, indicating that the Pax3-Tv-a model is a specific tool for the study of DIPG and that Pax3-expressing cells may represent a unique, regionally distinct cell of origin for DIPG.

In conclusion, we have described here novel populations of Pax3-expressing cells in the neonatal mouse brainstem and a novel GEMM of BSG that is initiated in these Pax3 cells. This model accurately represents the oligodendroglial/PDGFRA and H3-K27M subsets of DIPG and will be a valuable tool moving forward for DIPG research.

Supplementary data to this article can be found online at http://dx.doi.org/10.1016/j.neo.2015.12.002.

Acknowledgements

We would like to thank William Pavan, PhD, and Stacie Loftus, PhD, at the National Human Genome Research Institute for providing us with the Pax3-Tv-a mice, and Grigori Enikolopov, PhD, for the Nestin-CFPnuc transgenic mice. O. J. B. is supported by the Damon Runyon Cancer Research Foundation, U.S. Department of Defense, Rory David Deutsch Foundation, and Pediatric Brain Tumor Foundation. Research reported in this publication was supported by the National Institute of Neurological Disorders and Stroke of the National Institutes of Health under award number K02NS086917.

References

[1] Donaldson SS, Laningham F, and Fisher PG (2006). Advances toward an understanding of brainstem gliomas. *J Clin Oncol* **24**, 1266–1272.

[2] Hargrave D, Bartels U, and Bouffet E (2006). Diffuse brainstem glioma in children: critical review of clinical trials. *Lancet Oncol* **7**, 241–248.

[3] Khuong-Quang DA, Buczkowicz P, Rakopoulos P, Liu XY, Fontebasso AM, Bouffet E, Bartels U, Albrecht S, Schwartzentruber J, and Letourneau L, et al (2012). K27M mutation in histone H3.3 defines clinically and biologically distinct subgroups of pediatric diffuse intrinsic pontine gliomas. *Acta Neuropathol* **124**, 439–447.

[4] Schwartzentruber J, Korshunov A, Liu XY, Jones DT, Pfaff E, Jacob K, Sturm D, Fontebasso AM, Quang DA, and Tonjes M, et al (2012). Driver mutations in histone H3.3 and chromatin remodelling genes in paediatric glioblastoma. *Nature* **482**, 226–231.

[5] Sturm D, Witt H, Hovestadt V, Khuong-Quang D-A, Jones David TW, Konermann C, Pfaff E, Tönjes M, Sill M, and Bender S, et al (2012). Hotspot mutations in H3F3A and IDH1 define distinct epigenetic and biological subgroups of glioblastoma. *Cancer Cell* **22**, 425–437.

[6] Wu G, Broniscer A, McEachron TA, Lu C, Paugh BS, Becksfort J, Qu C, Ding L, Huether R, and Parker M, et al (2012). Somatic histone H3 alterations in pediatric diffuse intrinsic pontine gliomas and non-brainstem glioblastomas. *Nat Genet* **44**, 251–253.

[7] Castel D, Philippe C, Calmon R, Le Dret L, Truffaux N, Boddaert N, Pages M, Taylor KR, Saulnier P, and Lacroix L, et al (2015). Histone H3F3A and HIST1H3B K27M mutations define two subgroups of diffuse intrinsic pontine gliomas with different prognosis and phenotypes. *Acta Neuropathol* **130**(6), 815–827.

[8] Paugh BS, Broniscer A, Qu C, Miller CP, Zhang J, Tatevossian RG, Olson JM, Geyer JR, Chi SN, and da Silva NS, et al (2011). Genome-wide analyses identify recurrent amplifications of receptor tyrosine kinases and cell-cycle regulatory genes in diffuse intrinsic pontine glioma. *J Clin Oncol* **29**, 3999–4006.

[9] Paugh BS, Qu C, Jones C, Liu Z, Adamowicz-Brice M, Zhang J, Bax DA, Coyle B, Barrow J, and Hargrave D, et al (2010). Integrated molecular genetic profiling of pediatric high-grade gliomas reveals key differences with the adult disease. *J Clin Oncol* **28**, 3061–3068.

[10] Barrow J, Adamowicz-Brice M, Cartmill M, MacArthur D, Lowe J, Robson K, Brundler MA, Walker DA, Coyle B, and Grundy R (2011). Homozygous loss of ADAM3A revealed by genome-wide analysis of pediatric high-grade glioma and diffuse intrinsic pontine gliomas. *Neuro Oncol* **13**, 212–222.

[11] Paugh BS, Zhu X, Qu C, Endersby R, Diaz AK, Zhang J, Bax DA, Carvalho D, Reis RM, and Onar-Thomas A, et al (2013). Novel oncogenic PDGFRA mutations in pediatric high-grade gliomas. *Cancer Res* **73**, 6219–6229.

[12] Puget S, Philippe C, Bax DA, Job B, Varlet P, Junier M-P, Andreiuolo F, Carvalho D, Reis R, and Guerrini-Rousseau L, et al (2012). Mesenchymal transition and PDGFRA amplification/mutation are key distinct oncogenic events in pediatric diffuse intrinsic pontine gliomas. *PLoS One* **7**e30313.

[13] Zarghooni M, Bartels U, Lee E, Buczkowicz P, Morrison A, Huang A, Bouffet E, and Hawkins C (2010). Whole-genome profiling of pediatric diffuse intrinsic pontine gliomas highlights platelet-derived growth factor receptor and poly (ADP-ribose) polymerase as potential therapeutic targets. *J Clin Oncol* **28**, 1337–1344.

[14] Buczkowicz P, Hoeman C, Rakopoulos P, Pajovic S, Letourneau L, Dzamba M, Morrison A, Lewis P, Bouffet E, and Bartels U, et al (2014). Genomic analysis of diffuse intrinsic pontine gliomas identifies three molecular subgroups and recurrent activating ACVR1 mutations. *Nat Genet* **46**, 451–456.

[15] Fontebasso AM, Papillon-Cavanagh S, Schwartzentruber J, Nikbakht H, Gerges N, Fiset PO, Bechet D, Faury D, De Jay N, and Ramkissoon LA, et al (2014). Recurrent somatic mutations in ACVR1 in pediatric midline high-grade astrocytoma. *Nat Genet* **46**, 462–466.

[16] Taylor KR, Mackay A, Truffaux N, Butterfield YS, Morozova O, Philippe C, Castel D, Grasso CS, Vinci M, and Carvalho D, et al (2014). Recurrent activating ACVR1 mutations in diffuse intrinsic pontine glioma. *Nat Genet* **46**, 457–461.

[17] Wu G, Diaz AK, Paugh BS, Rankin SL, Ju B, Li Y, Zhu X, Qu C, Chen X, and Zhang J, et al (2014). The genomic landscape of diffuse intrinsic pontine glioma and pediatric non-brainstem high-grade glioma. *Nat Genet* **46**, 444–450.

[18] Monje M, Mitra SS, Freret ME, Raveh TB, Kim J, Masek M, Attema JL, Li G, Haddix T, and Edwards MSB, et al (2011). Hedgehog-responsive candidate cell of origin for diffuse intrinsic pontine glioma. *Proc Natl Acad Sci* **108**, 4453–4458.

[19] Fischbein NJ, Prados MD, Wara W, Russo C, Edwards MS, and Barkovich AJ (1996). Radiologic classification of brain stem tumors: correlation of magnetic resonance imaging appearance with clinical outcome. *Pediatr Neurosurg* **24**, 9–23.

[20] Tate MC, Lindquist RA, Nguyen T, Sanai N, Barkovich AJ, Huang EJ, Rowitch DH, and Alvarez-Buylla A (2015). Postnatal growth of the human pons: a morphometric and immunohistochemical analysis. *J Comp Neurol* **523**, 449–462.

[21] Barton KL, Misuraca K, Cordero F, Dobrikova E, Min HD, Gromeier M, Kirsch DG, and Becher OJ (2013). PD-0332991, a CDK4/6 inhibitor, significantly prolongs survival in a genetically engineered mouse model of brainstem glioma. *PLoS One* **8**e77639.

[22] Becher OJ, Hambardzumyan D, Walker TR, Helmy K, Nazarian J, Albrecht S, Hiner RL, Gall S, Huse JT, and Jabado N, et al (2010). Preclinical evaluation of radiation and perifosine in a genetically and histologically accurate model of brainstem glioma. *Cancer Res* **70**, 2548–2557.

[23] Lewis PW, Muller MM, Koletsky MS, Cordero F, Lin S, Banaszynski LA, Garcia BA, Muir TW, Becher OJ, and Allis CD (2013). Inhibition of PRC2 activity by a gain-of-function H3 mutation found in pediatric glioblastoma. *Science* **340**, 857–861.

[24] Misuraca KL, Barton KL, Chung A, Diaz AK, Conway SJ, Corcoran DL, Baker SJ, and Becher OJ (2014). Pax3 expression enhances PDGF-B-induced brainstem gliomagenesis and characterizes a subset of brainstem glioma. *Acta Neuropathol Commun* **2**, 134.

[25] Hou L, Loftus SK, Incao A, Chen A, and Pavan WJ (2004). Complementation of melanocyte development in SOX10 mutant neural crest using lineage-directed gene transfer. *Dev Dyn* **229**, 54–62.

[26] Becher OJ and Holland EC (2010). Evidence for and against regional differences in neural stem and progenitor cells of the CNS. *Genes Dev* **24**, 2233–2238.

[27] Encinas JM, Vaahtokari A, and Enikolopov G (2006). Fluoxetine targets early progenitor cells in the adult brain. *Proc Natl Acad Sci U S A* **103**, 8233–8238.

[28] Hoffman RM (2015). Patient-derived orthotopic xenografts: better mimic of metastasis than subcutaneous xenografts. *Nat Rev Cancer* **15**, 451–452.

[29] Misuraca KL, Cordero FJ, and Becher OJ (2015). Pre-clinical models of diffuse intrinsic pontine glioma. *Front Oncol* **5**, 172.

[30] Bang AG, Papalopulu N, Goulding MD, and Kintner C (1999). Expression of Pax-3 in the lateral neural plate is dependent on a Wnt-mediated signal from posterior nonaxial mesoderm. *Dev Biol* **212**, 366–380.

[31] Bang AG, Papalopulu N, Kintner C, and Goulding MD (1997). Expression of Pax-3 is initiated in the early neural plate by posteriorizing signals produced by the organizer and by posterior non-axial mesoderm. *Development* **124**, 2075–2085.

[32] Pani L, Horal M, and Loeken MR (2002). Rescue of neural tube defects in Pax-3–deficient embryos by p53 loss of function: implications for Pax-3–dependent development and tumorigenesis. *Genes Dev* **16**, 676–680.

[33] Tanabe Y and Jessell TM (1996). Diversity and pattern in the developing spinal cord. *Science* **274**, 1115–1123.

[34] (2013). Allen Institute for Brain Science. Allen Developing Mouse Brain Atlas. Editor (ed)^(eds): City.

[35] Ballester LY, Wang Z, Shandilya S, Miettinen M, Burger PC, Eberhart CG, Rodriguez FJ, Raabe E, Nazarian J, and Warren K, et al (2013). Morphologic characteristics and immunohistochemical profile of diffuse intrinsic pontine gliomas. *Am J Surg Pathol* **37**, 1357–1364.

[36] Chan KM, Fang D, Gan H, Hashizume R, Yu C, Schroeder M, Gupta N, Mueller S, James CD, and Jenkins R, et al (2013). The histone H3.3K27M mutation in pediatric glioma reprograms H3K27 methylation and gene expression. *Genes Dev* **27**, 985–990.

[37] Funato K, Major T, Lewis PW, Allis CD, and Tabar V (2014). Use of human embryonic stem cells to model pediatric gliomas with H3.3K27M histone mutation. *Science* **346**, 1529–1533.

[38] Subashi E, Cordero FJ, Halvorson KG, Qi Y, Nouls JC, Becher OJ, and Allan Johnson G (2015). Tumor location, but not H3.3K27M, significantly influences the blood-brain-barrier permeability in a genetic mouse model of pediatric high-grade glioma. *J Neurooncol* [Epub ahead of print].

[39] Sharma MK, Mansur DB, Reifenberger G, Perry A, Leonard JR, Aldape KD, Albin MG, Emnett RJ, Loeser S, and Watson MA, et al (2007). Distinct genetic signatures among pilocytic astrocytomas relate to their brain region origin. *Cancer Res* **67**, 890–900.